Electronic Supplementary Information

Engineering dielectric constants in organic semiconductors

Ardalan Armin, Dani M. Stoltzfus, Jenny E. Donaghey, Andrew J. Clulow, Ravi Chandra Raju Nagiri, Paul L. Burn,* Ian R. Gentle, Paul Meredith[#]

[a]Centre for Organic Photonics & Electronics, School of Chemistry and Molecular Biosciences and School of Mathematics and Physics, The University of Queensland, St Lucia Campus, Brisbane 4072 (Australia)

[#] Now at: Department of Physics, Swansea University, Singleton Park, Swansea SA2 8PP, Wales, United Kingdom

*Email: p.burn2@uq.edu.au; meredith@physics.uq.edu.au

Contents

1. Effect of excess energy on the internal quantum efficiency

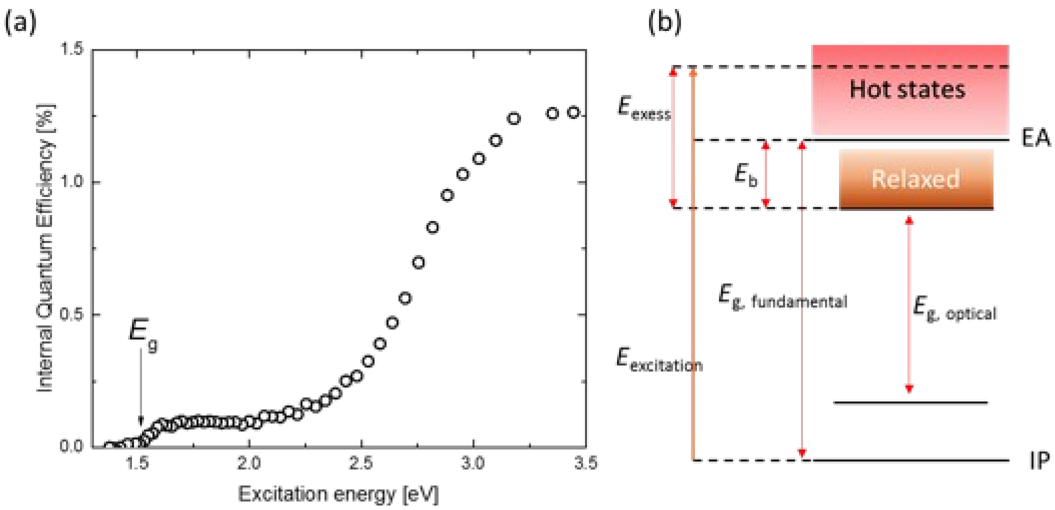

c

Figure S1. a) Internal quantum efficiency (IQE) of a PCPDTBT homojunction cell with the structure ITO/PEDOT/PCPDTBT/Sm:Al. In comparison to heterojunction cells that often exhibit spectrally flat efficiency, a substantial excess energy dependent charge generation can be observed when the excess energy is sufficiently large (> binding energy E_b). b) An energy diagram to elucidate the energy gap (E_g fundamental and optical), exciton binding energy (E_b) and the excess energy (E_{excess}). EA and IP denote electron affinity and ionization potential respectively.

2. NMR spectra of key compounds

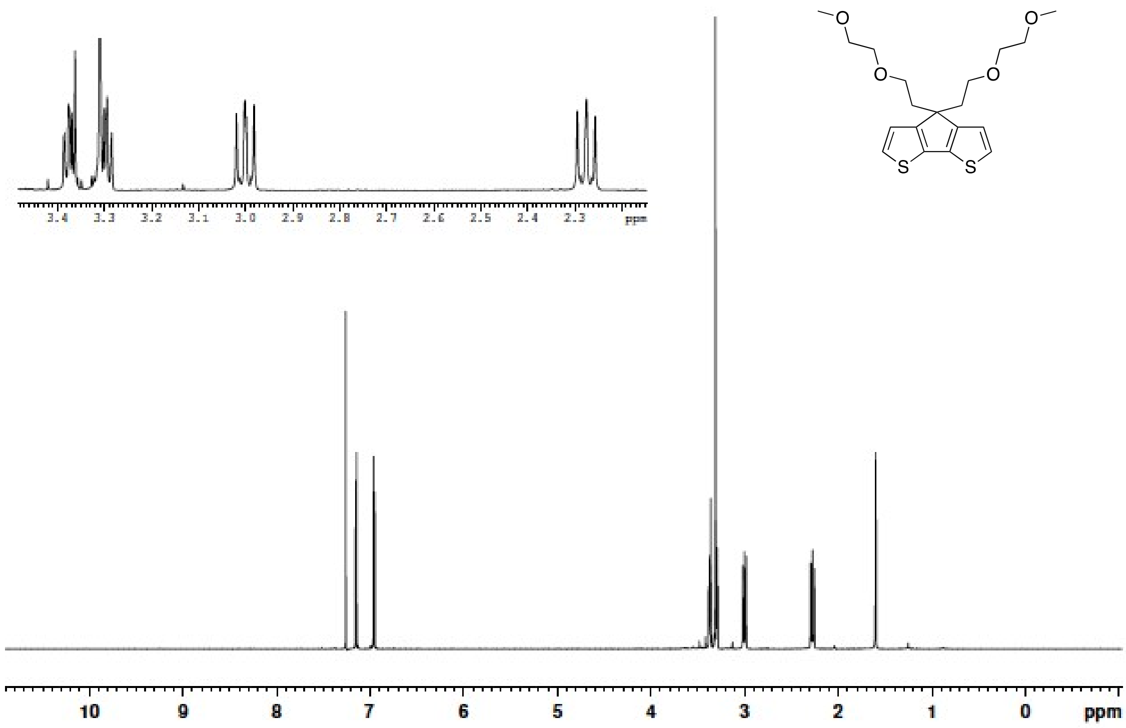

Figure S2. ^{1}H NMR spectrum of **4**

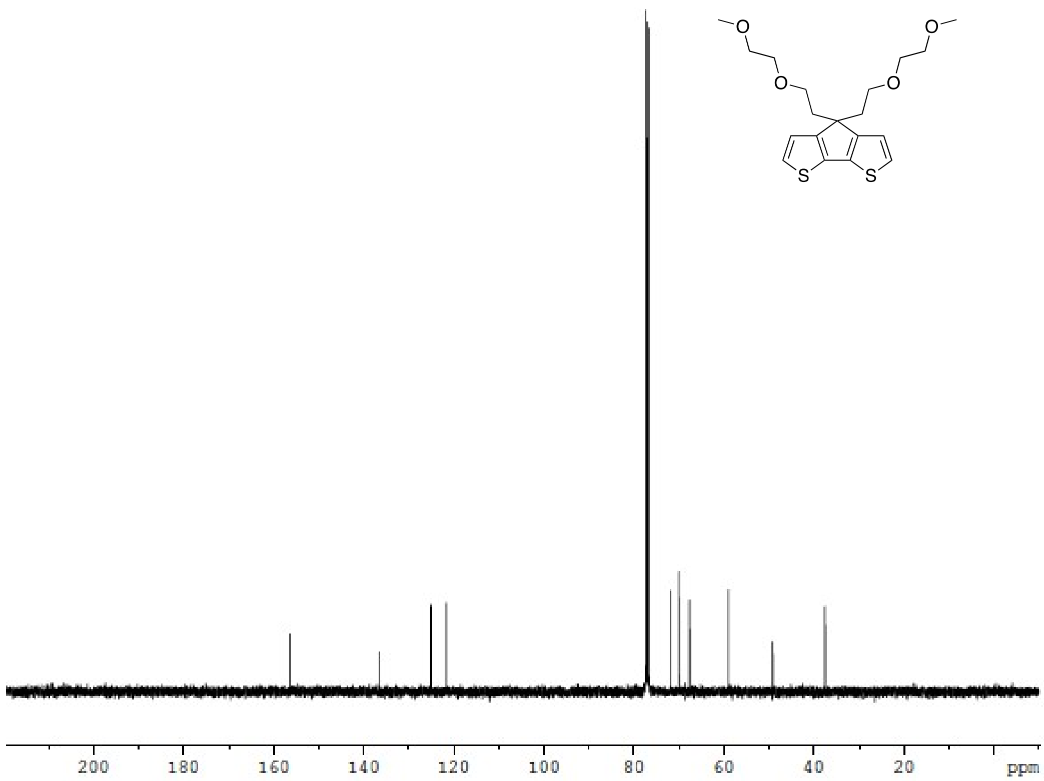

Figure S3. ^{13}C NMR spectrum of **4**

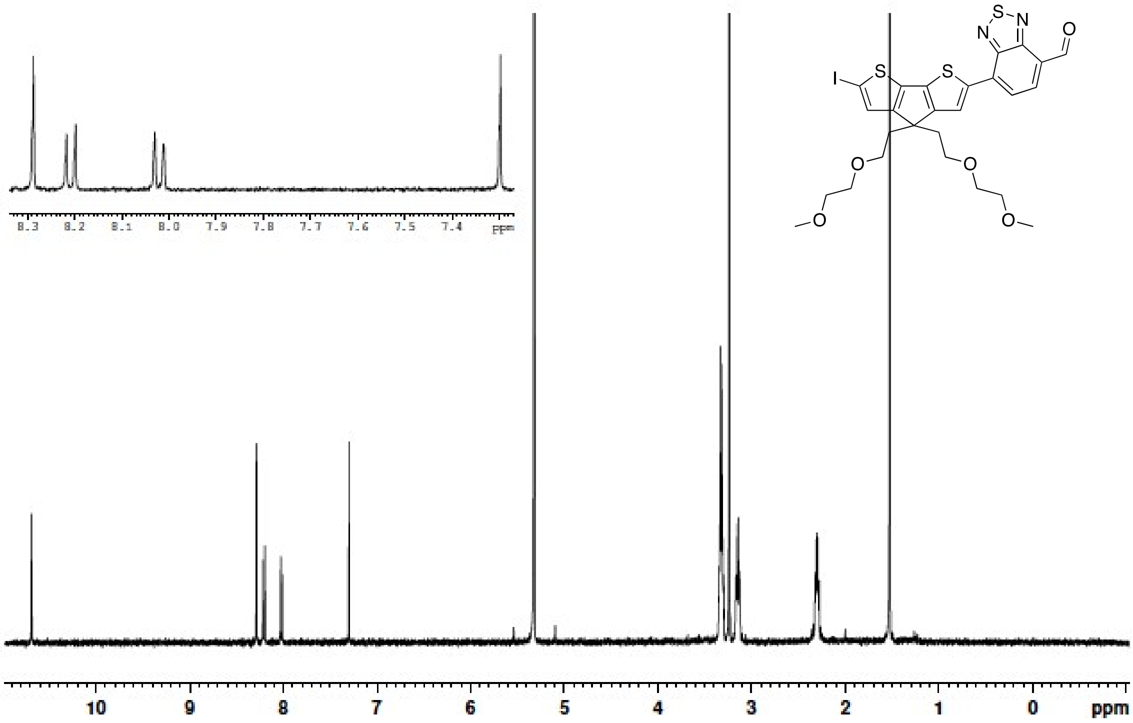

Figure S4. ^{1}H NMR spectrum of **2a**

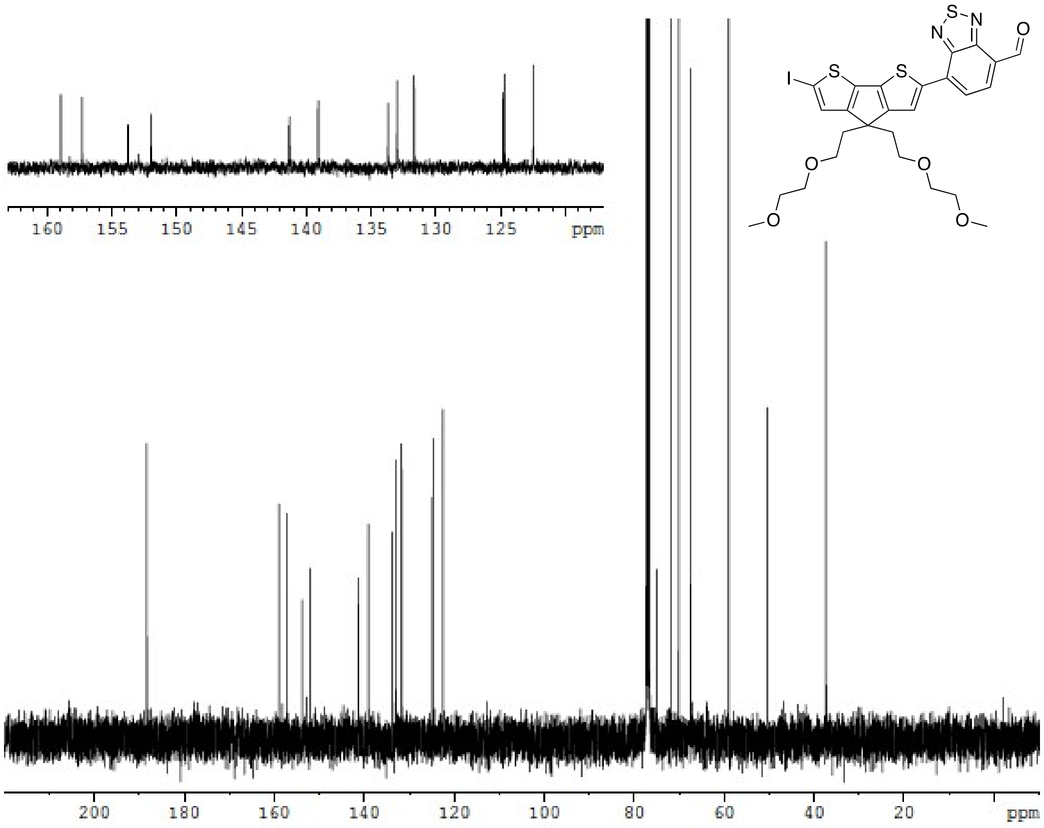

Figure S5. [13]C NMR spectrum of **2a**

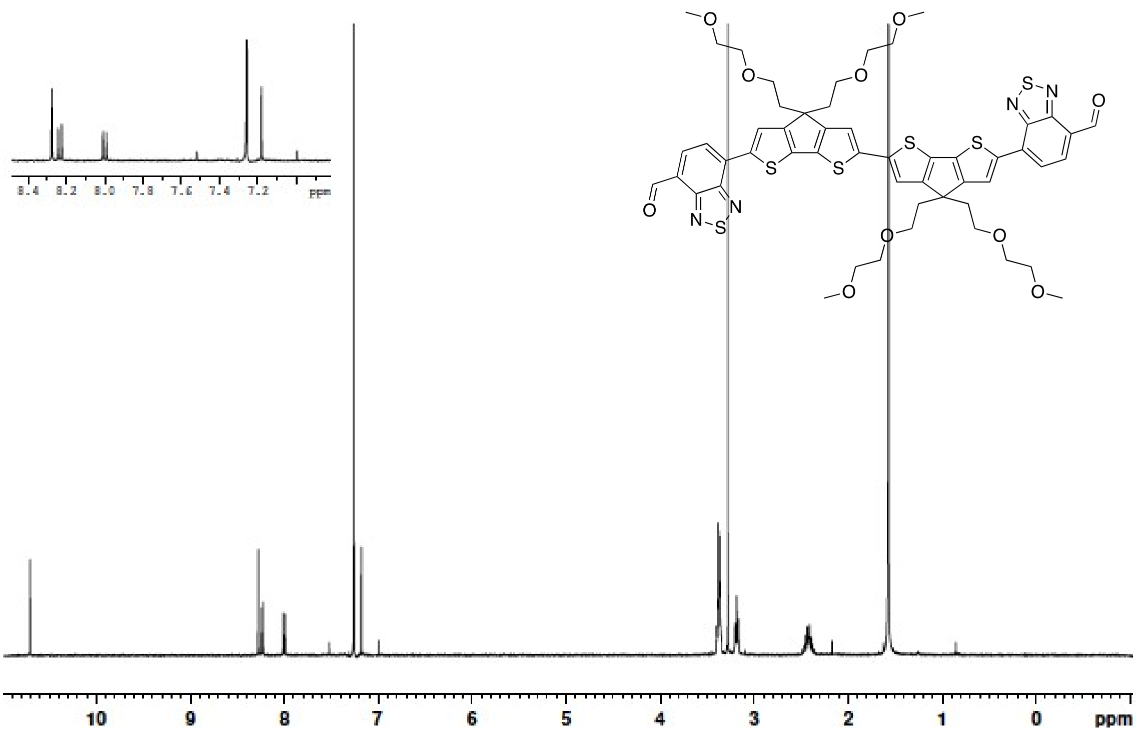

Figure S6. [1]H NMR spectrum of **3a**

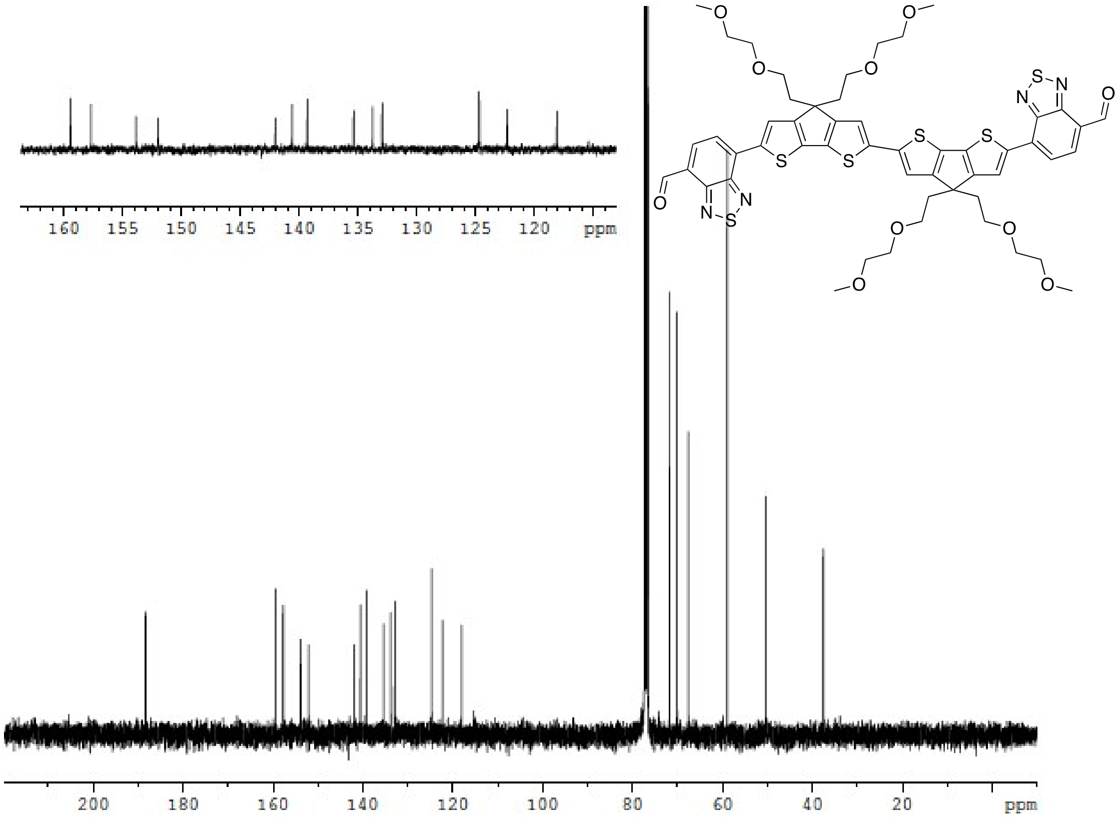

. Figure S7. ^{13}C NMR spectrum of **3a**

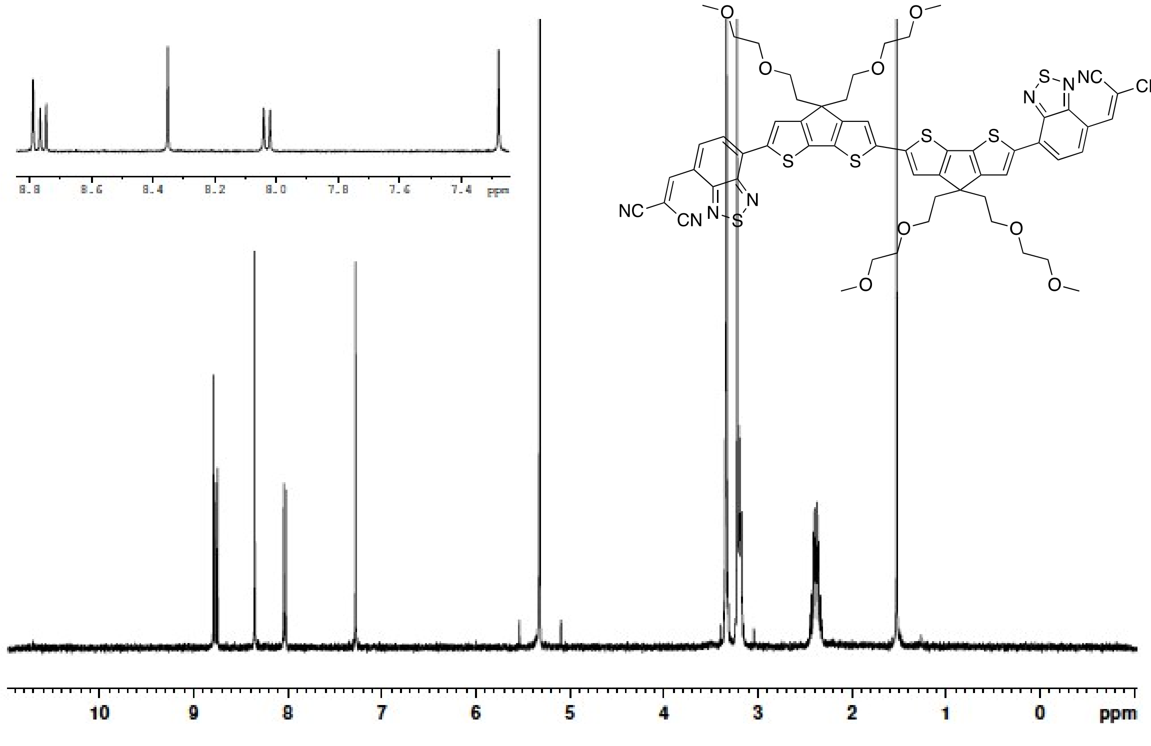

Figure S8. ^{1}H NMR spectrum of **DG**

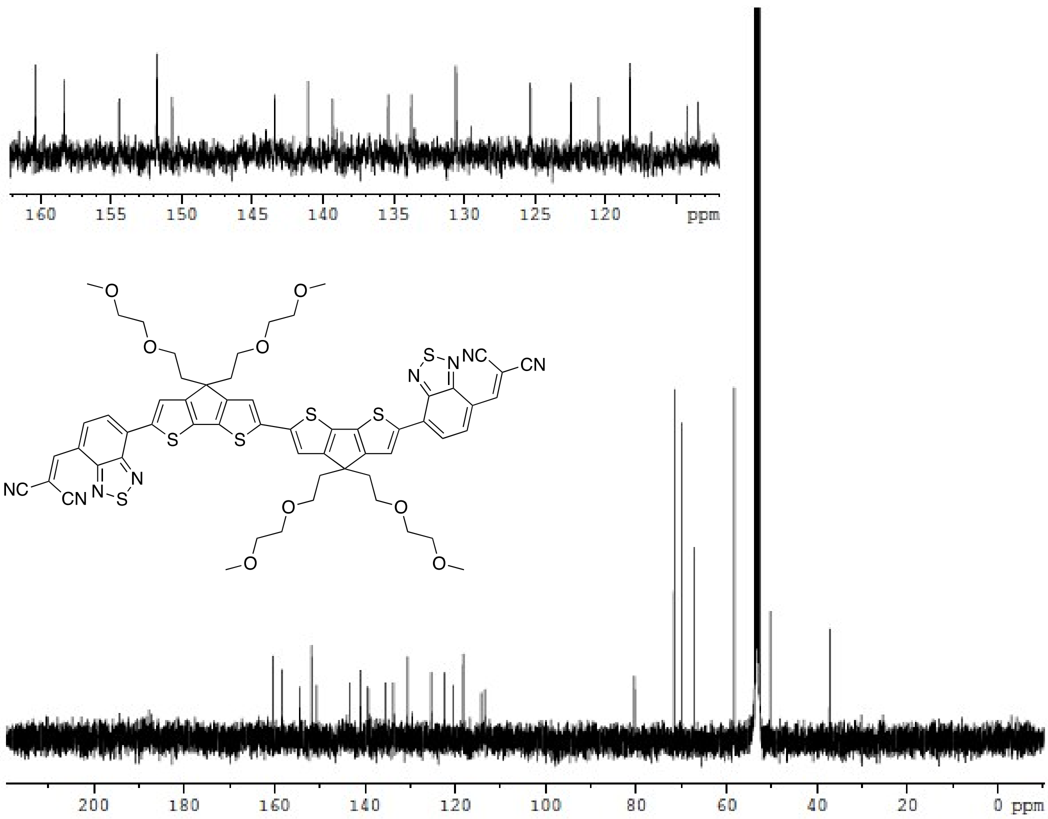

Figure S9. ^{13}C NMR spectrum of **DG**

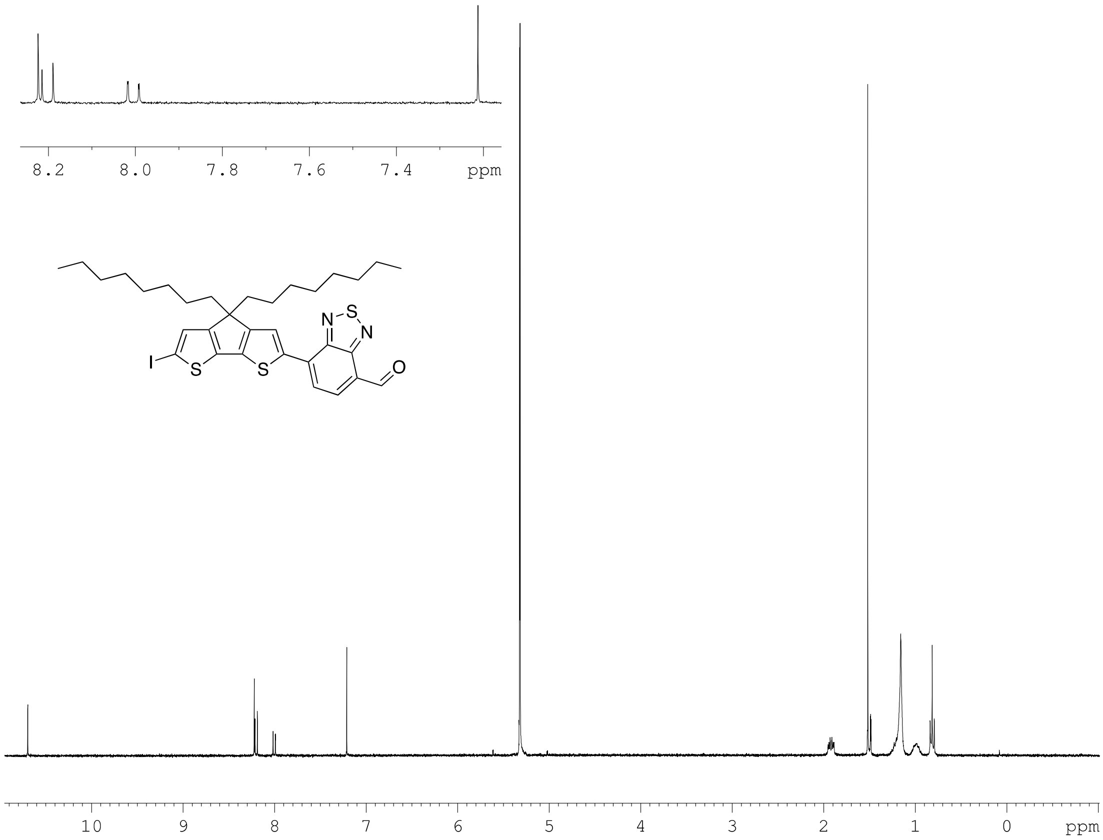

Figure S10. ^{1}H NMR spectrum of **2b**

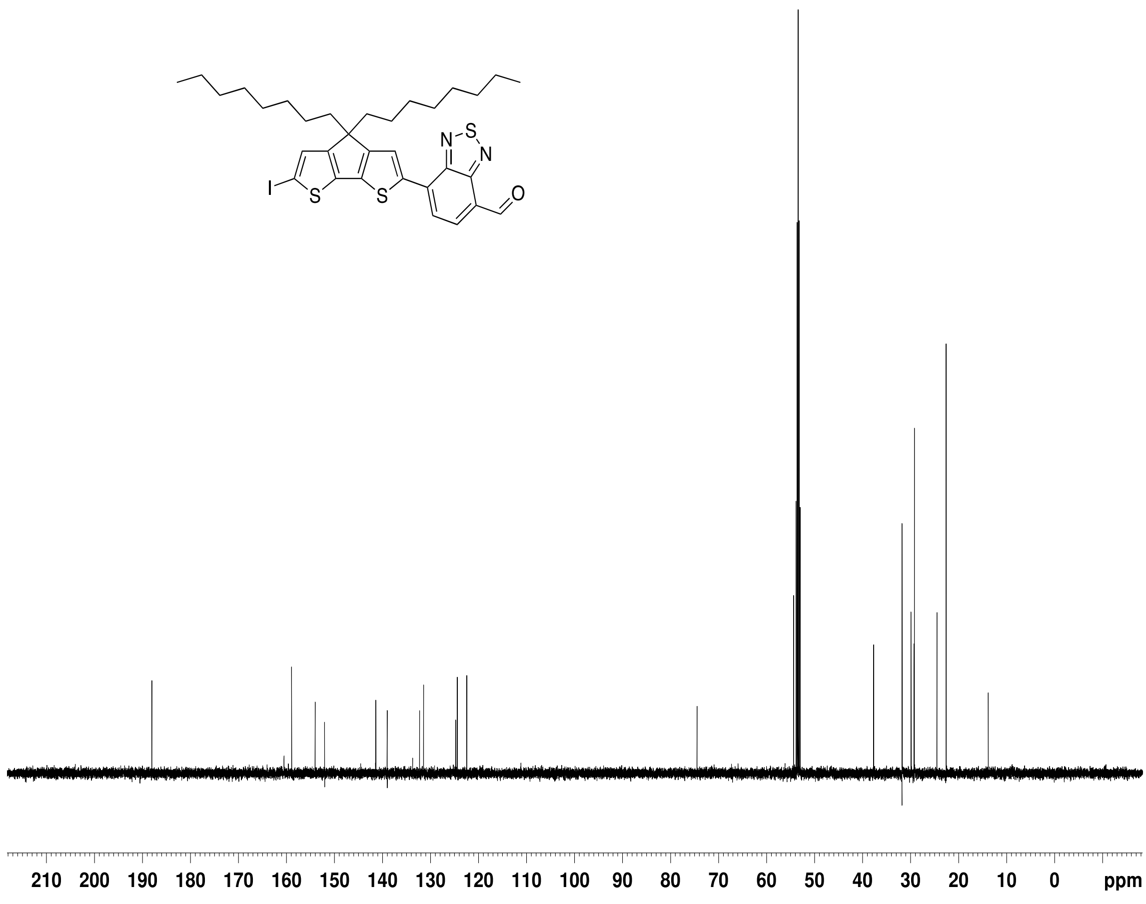

Figure S11. ^{13}C NMR spectrum of **2b**

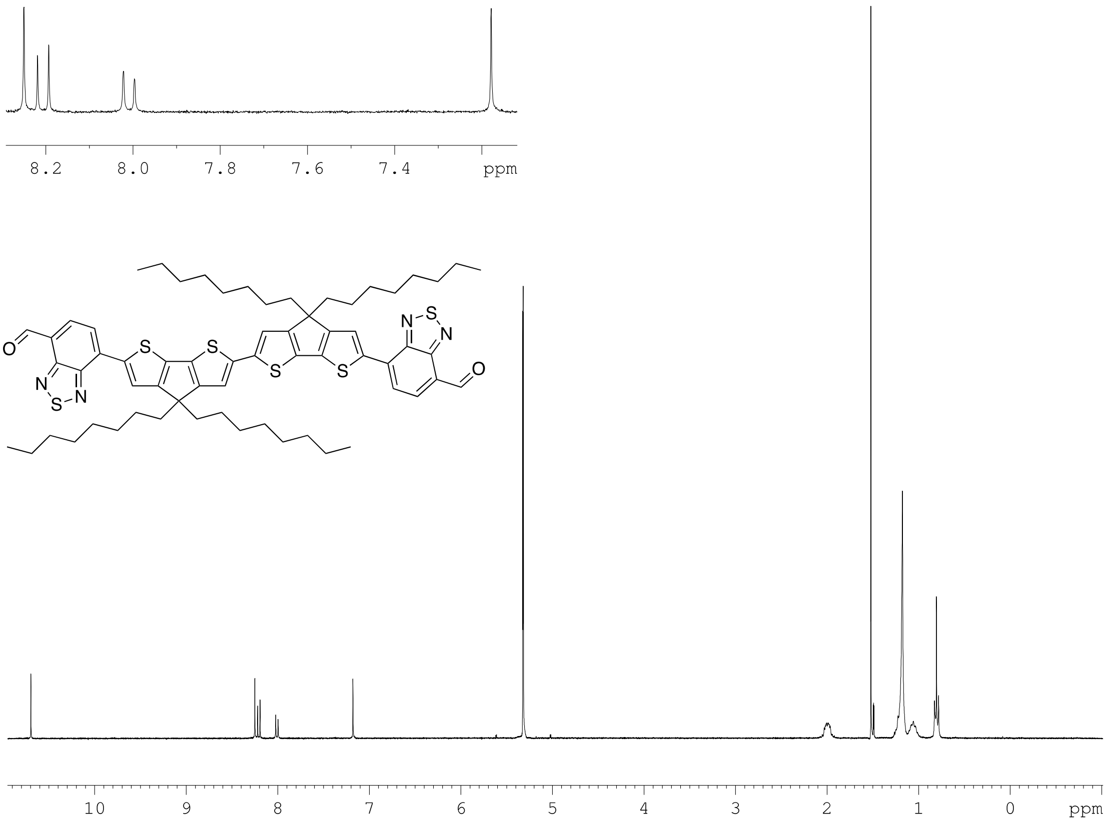

Figure S12. ^{1}H NMR spectrum of **3b**

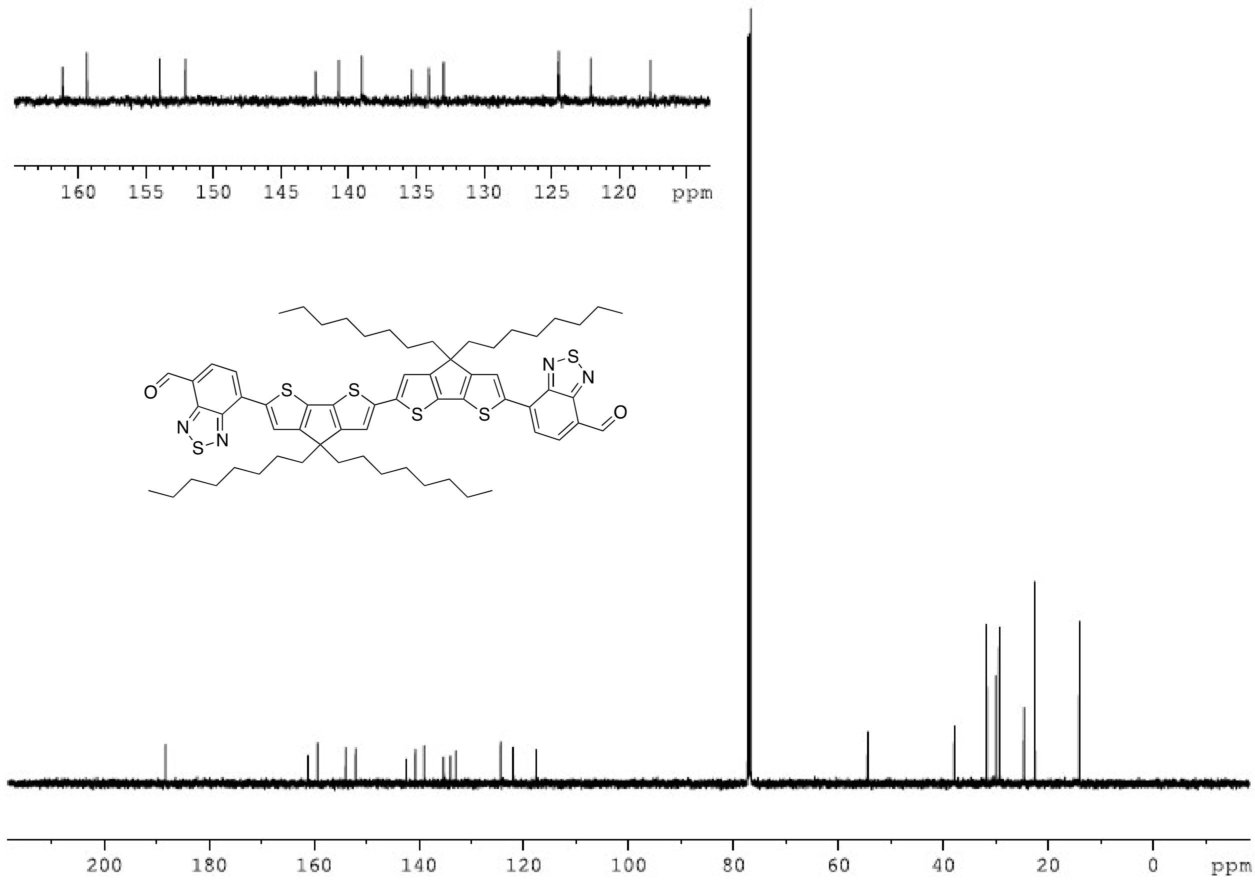

Figure S13. ^{13}C NMR spectrum of **3b**

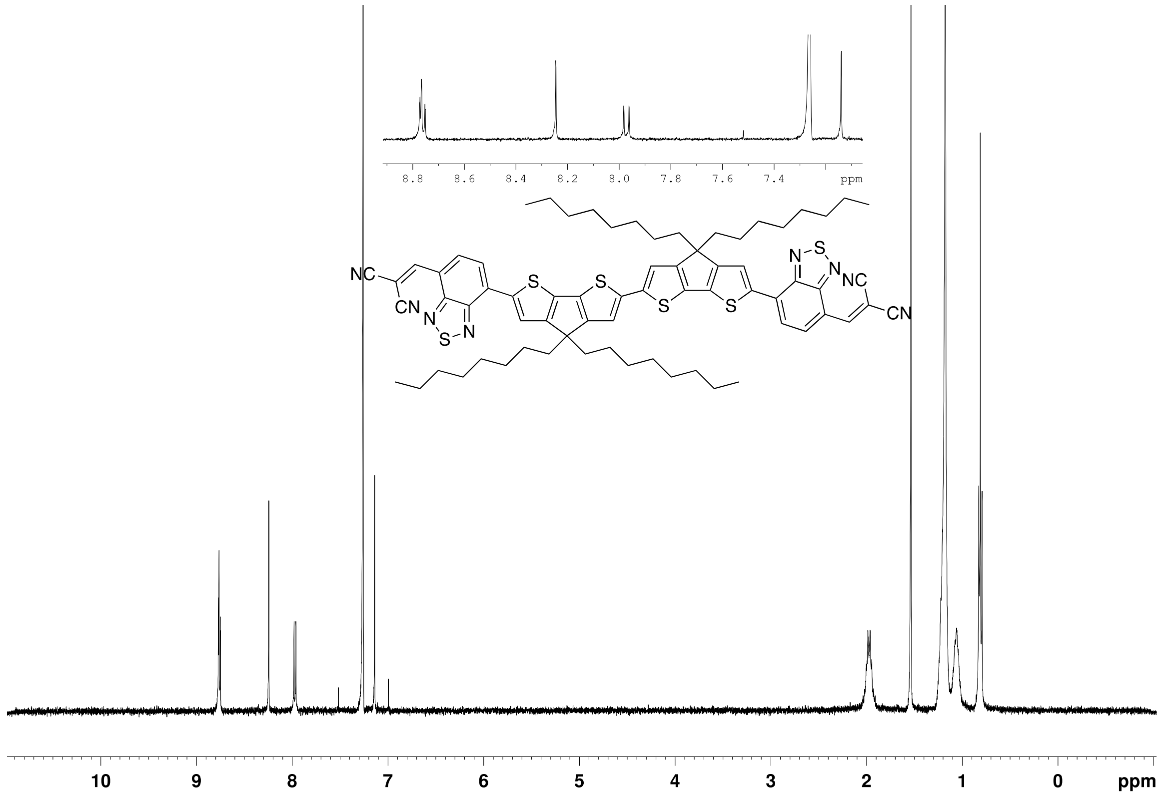

Figure S14. ^{1}H NMR spectrum of **DA**

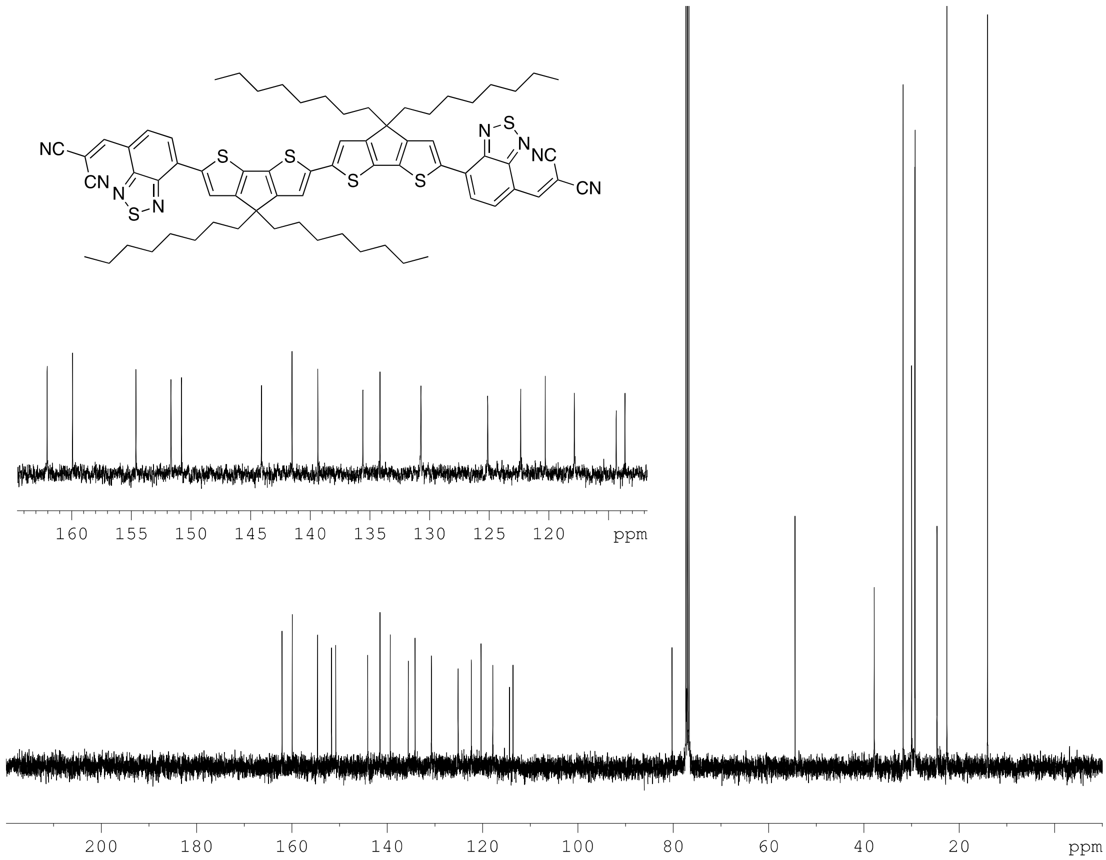

Figure S15. ^{13}C NMR spectrum of **DA**

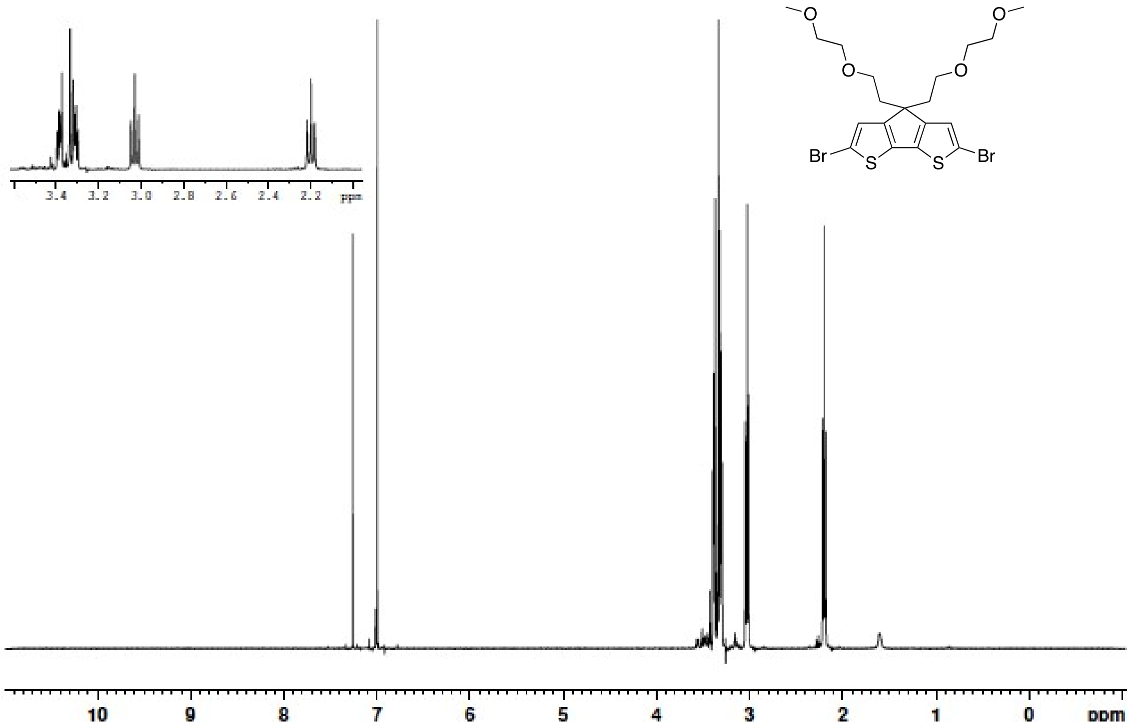

Figure S16. ^{1}H NMR spectrum of **5**

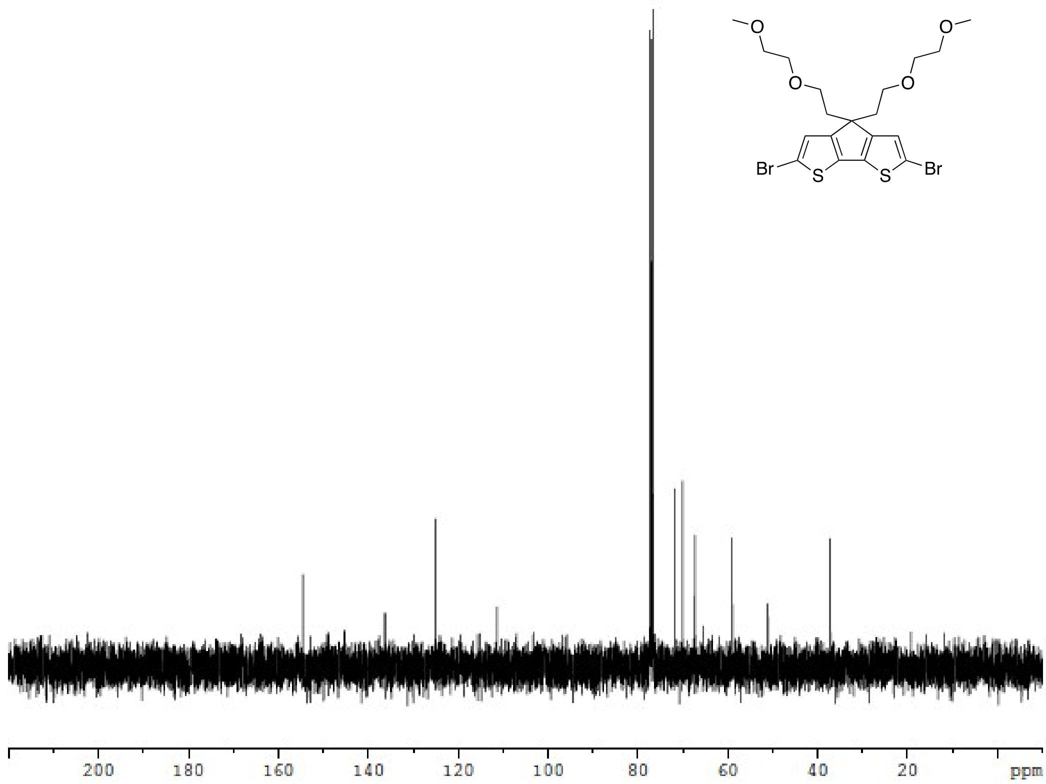

Figure S17. ^{13}C NMR spectrum of **5**

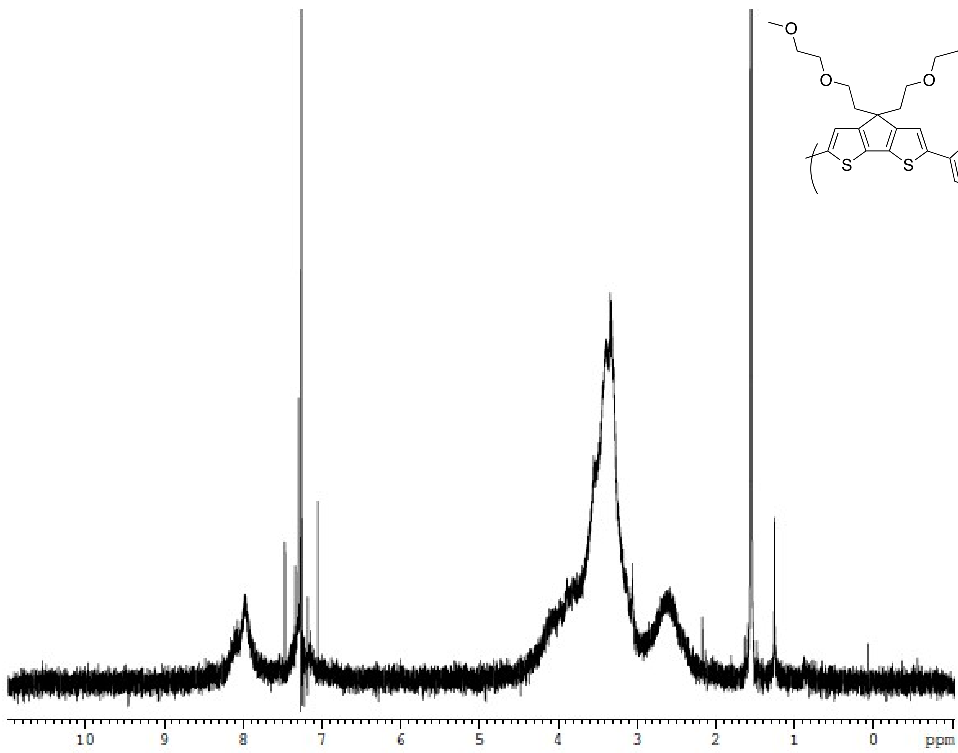

Figure S18. ^{1}H NMR spectrum of **PG**

3. Differential Scanning Calorimetry (DSC)

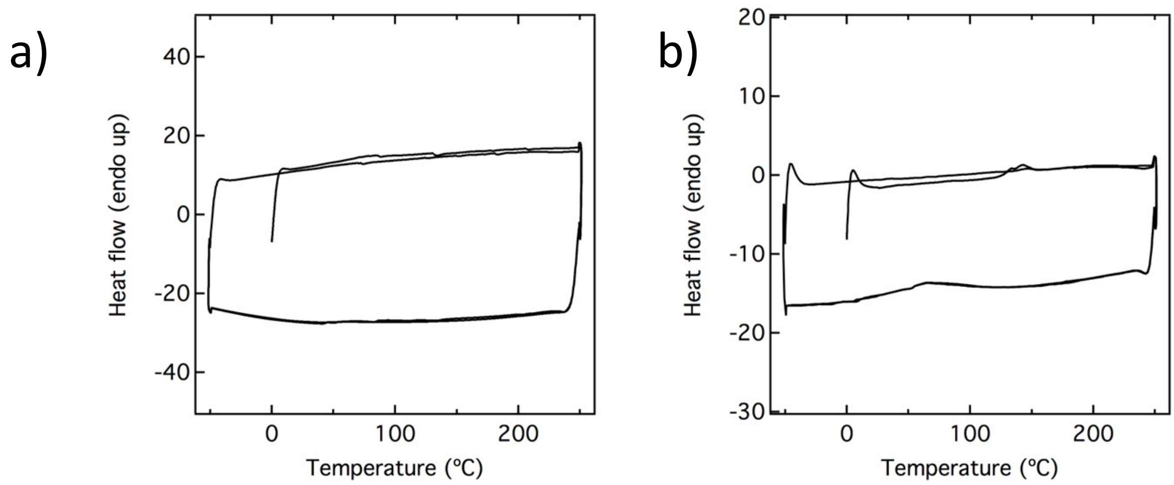

Figure S19. DSC thermograms of a) **PG** and b) **PCPDTBT**. Scan rate is 100 °C min^{-1}

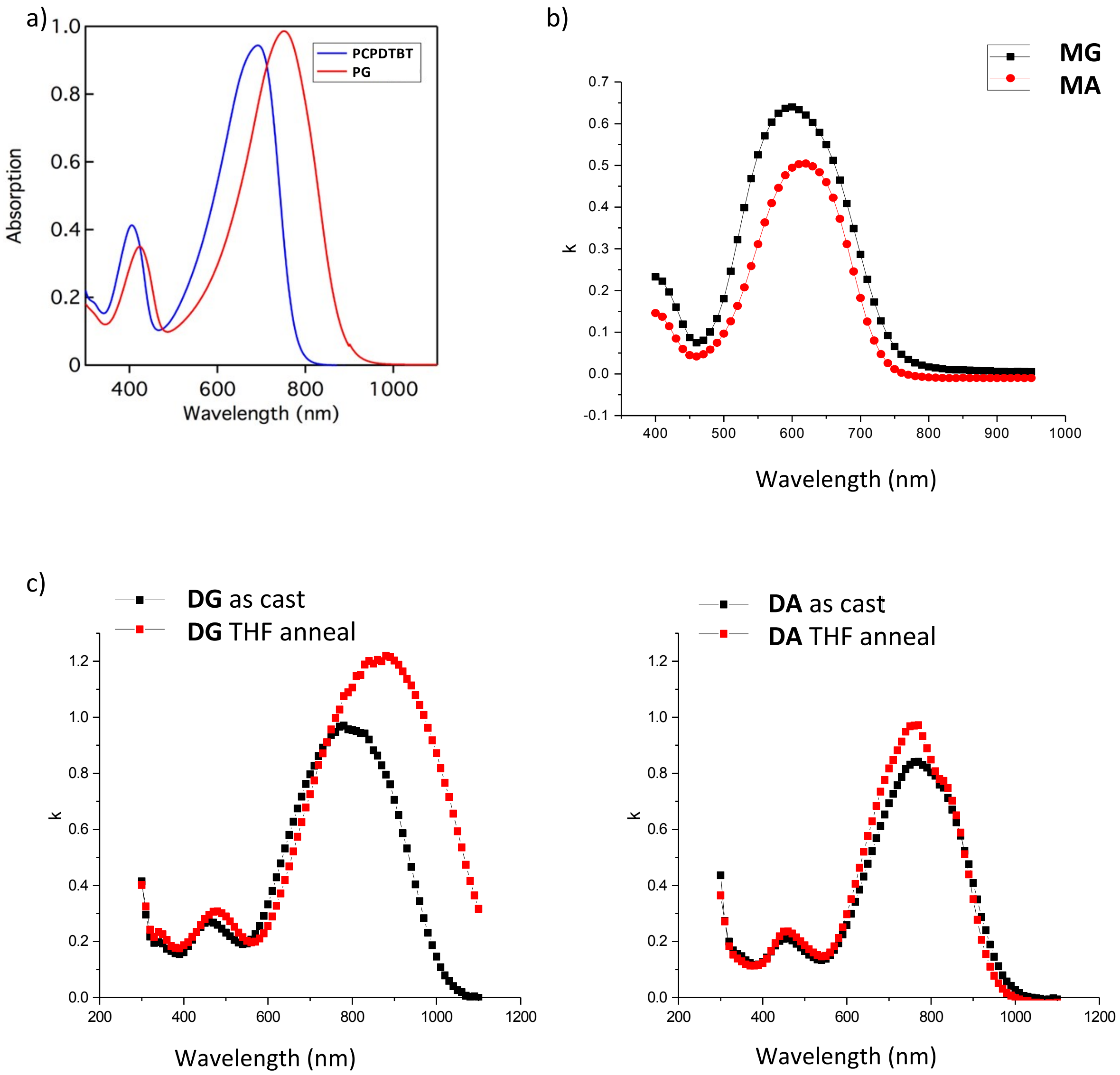

Figure S20. a) Solution absorption spectra of **PG** and **PCPDTBT** at the same weight/volume and solid state extinction coefficients (k) as a function of wavelength (WL) for b) Monomers and c) Dimers.

4. Photoluminescence spectra

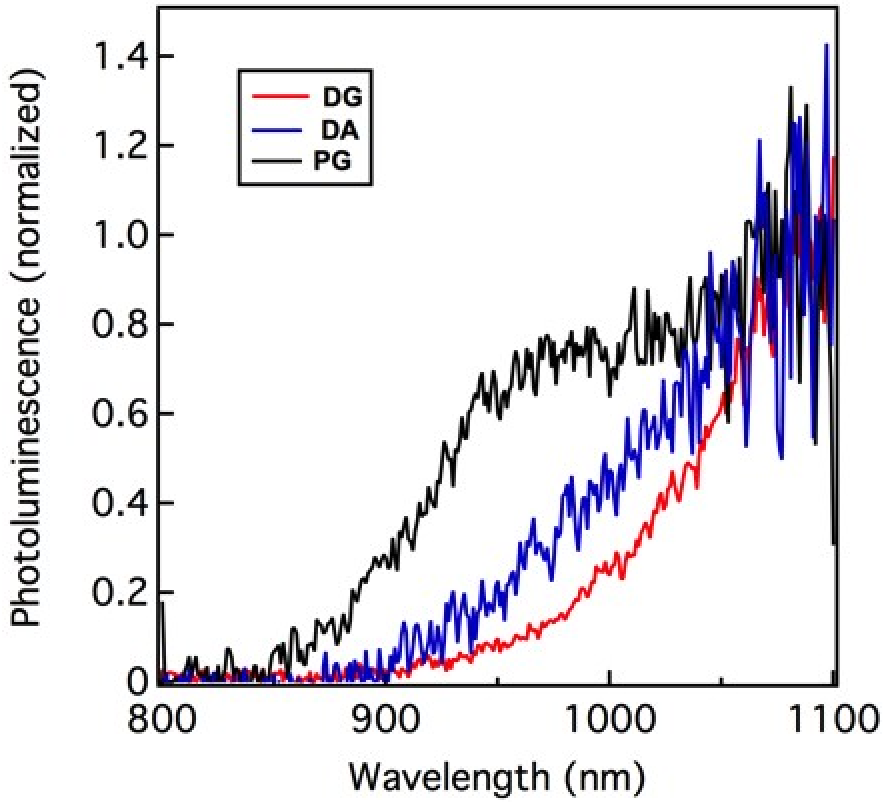

Figure S21. PL spectra of **DG**, **DA** and **PG** in thin films spin-coated from chloroform onto fused silica.

5. Optical gap

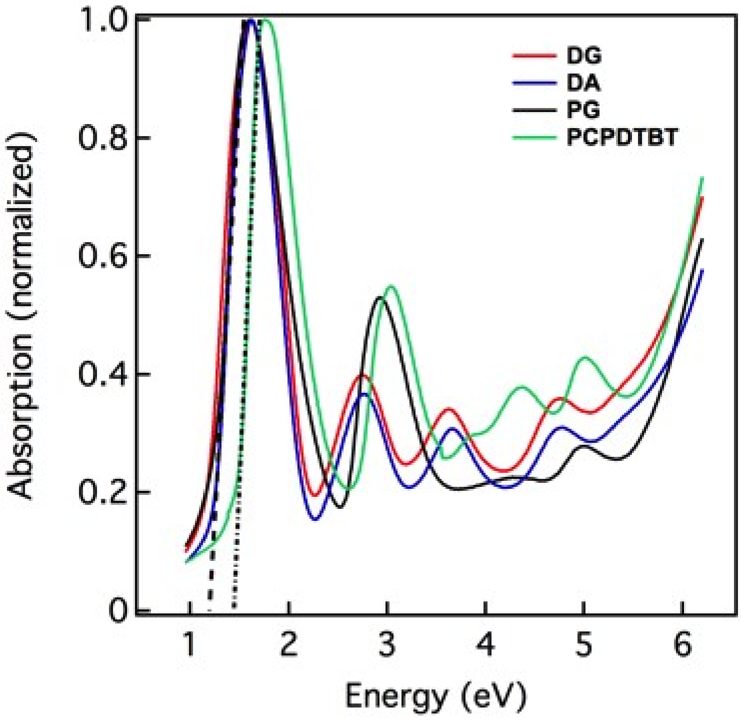

Figure S22. Estimation of the optical gap of **DG**, **DA** and **PG** (~ 1.2 eV) and **PCPDTBT** (~1.5 eV) in thin films spin-coated from chloroform onto fused silica.

6. X-ray analysis

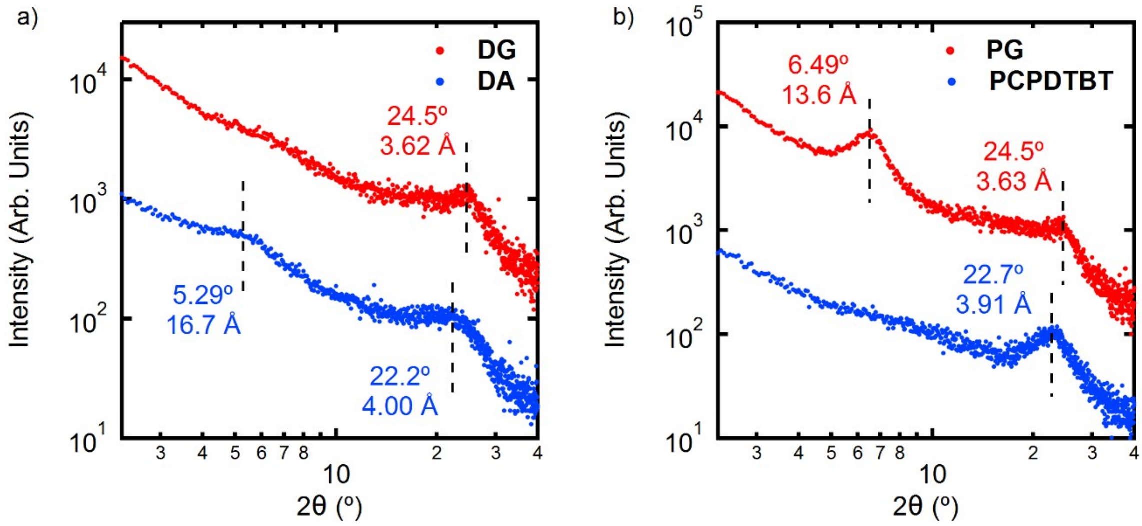

Figure S23. Grazing-incidence diffractograms of a) **DG** and **DA**; b) **PG** and **PCPDTBT** films spin-coated from chloroform onto silicon substrates. The red traces have been offset by a factor of 10 for clarity.

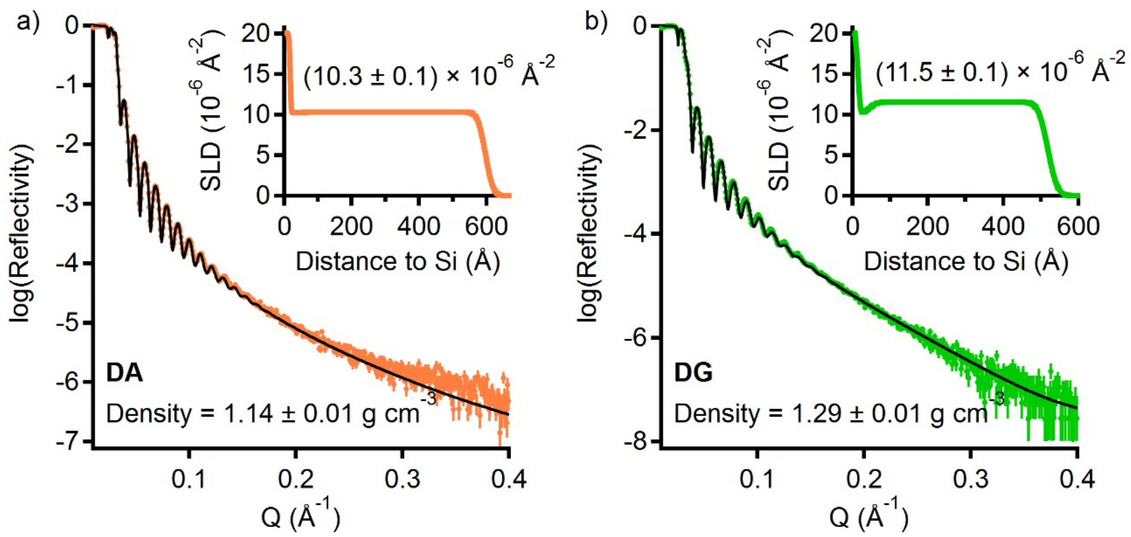

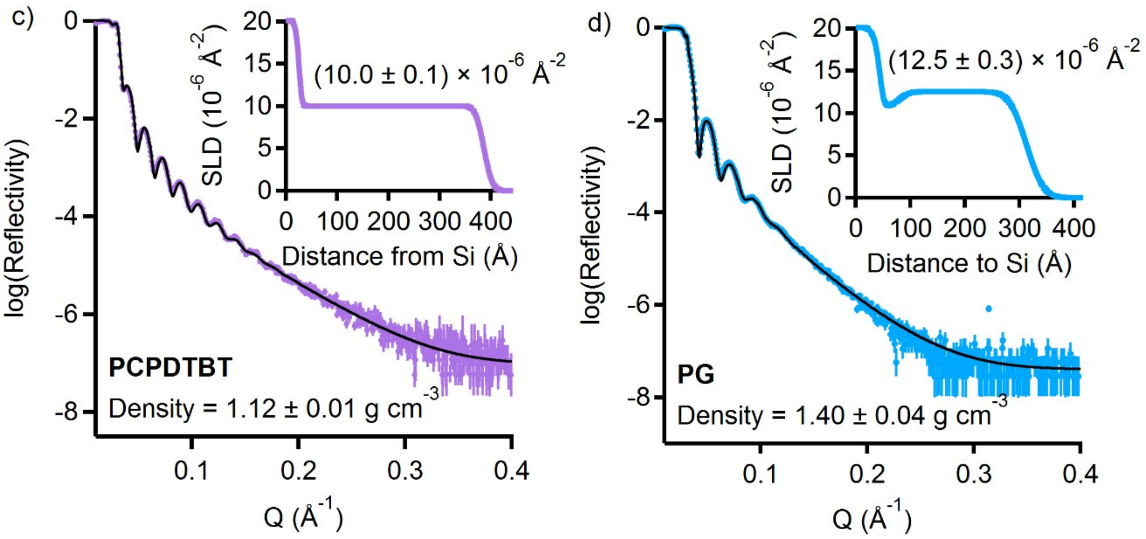

Figure S24. XRR profiles and corresponding SLD *versus* thickness plots (inserts) for a) **DA**, b) **DG**, c) **PCPDTBT** and d) **PG**. Individual points represent recorded data and solid black lines indicate the fitting curves. Films were spin-coated from chloroform onto silicon substrates.

7. Cyclic voltammetry (CV)

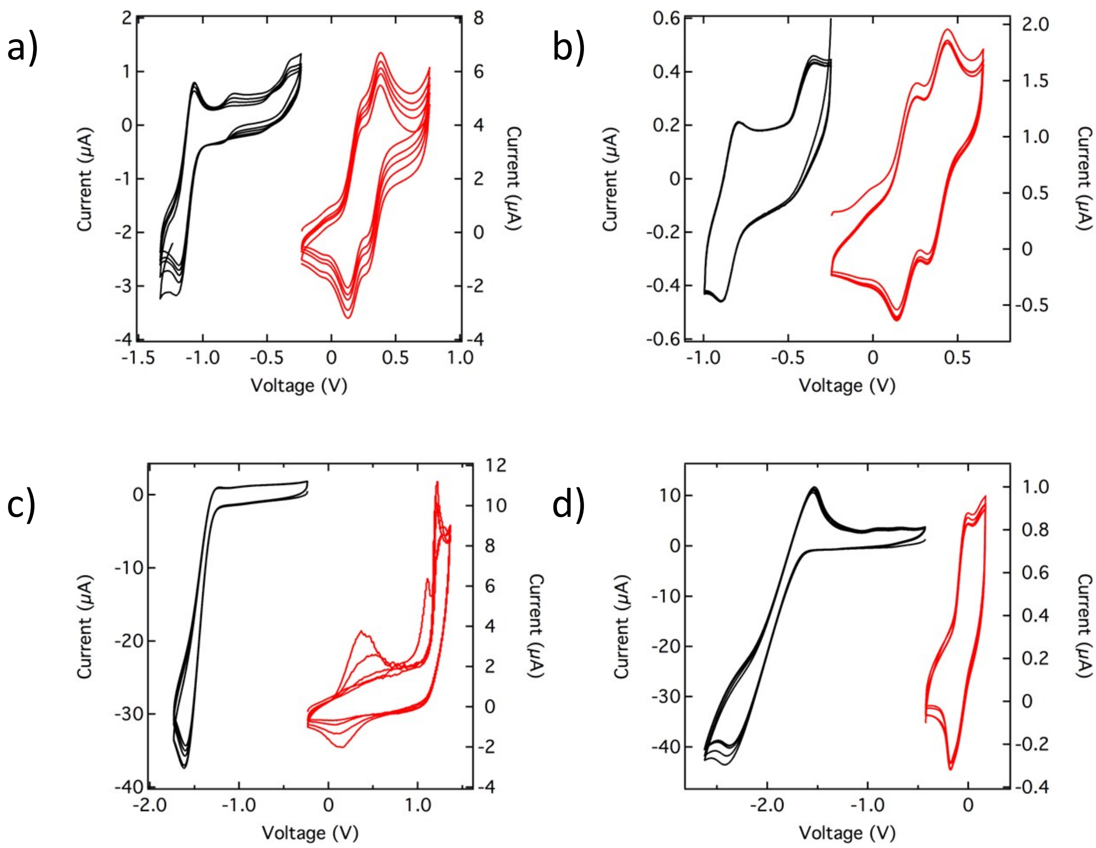

Figure S25. Cyclic voltammograms (first reduction and oxidations - 10 cycles) of a) **DG**; b) **DA**; c) **PG** and d) **PCPDTBT**.

8. SCLC

Hole/electron mobility measurements were conducted by measuring the Space-Charge-Limited-Current (SCLC) and employing the Mott-Gurney law and Poole-Frenkel models:

$$J = E\sigma + \frac{9}{8}\varepsilon_0\varepsilon_r\mu\frac{V^2}{d^3}e^{\sqrt{\frac{E}{E_0}}},$$

where ε_0, ε_r, μ, E, σ, d and E_0 are the vacuum permittivity, relative permittivity, mobility, electric field, conductivity, film thickness, and field dependence coefficient, respectively. The diode structure ITO/MoOx/semiconductor/MoOx/Ag was used for hole only devices and ITO/Al/semiconductor/Al for electron only devices.

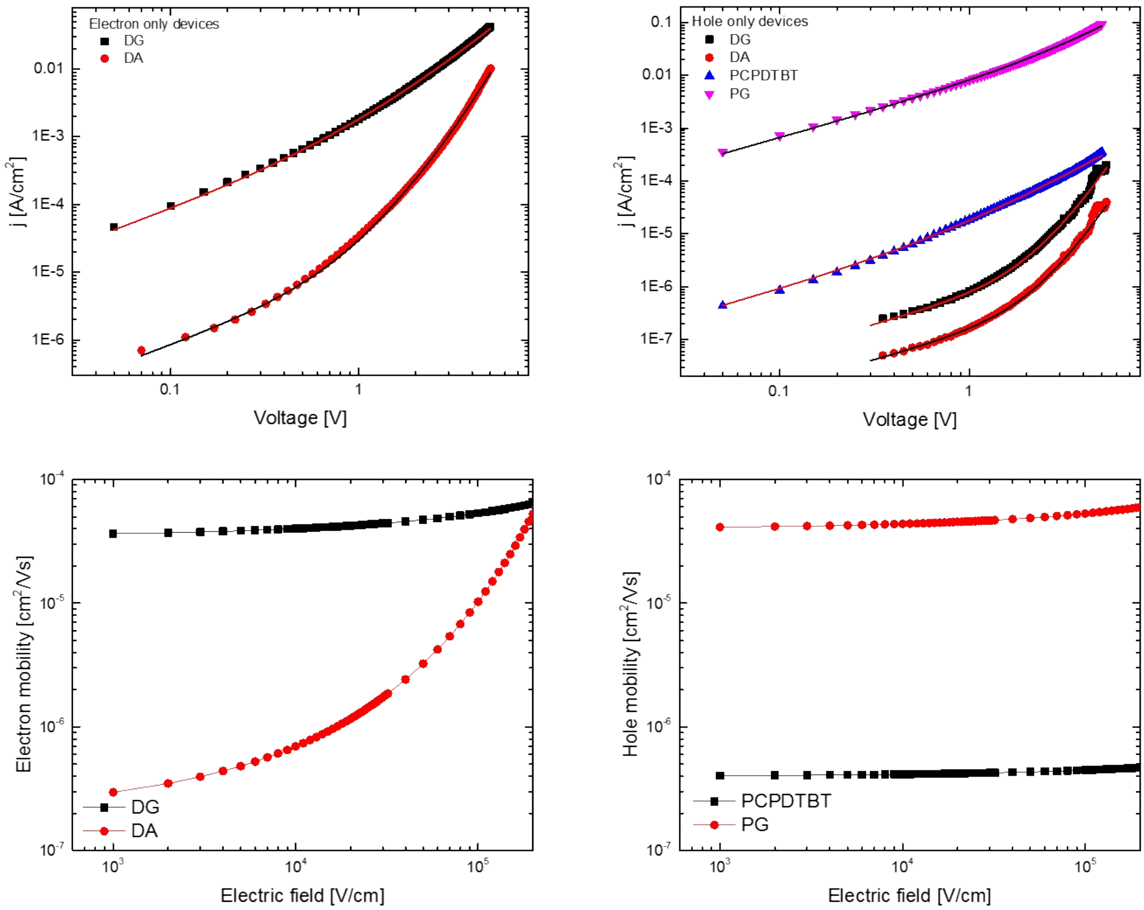

Figure S26. Current density-Voltage (*J-V*) curves of a) electron only devices of **DG** and **DA**; b) hole only devices of **DG**, **DA**, **PCPDTBT** and **PG**; c) electric field dependent mobility of **DG** and **DA** and d) electric field dependent mobility of **PCPDTBT** and **PG**.

9. Homojunction OPV data

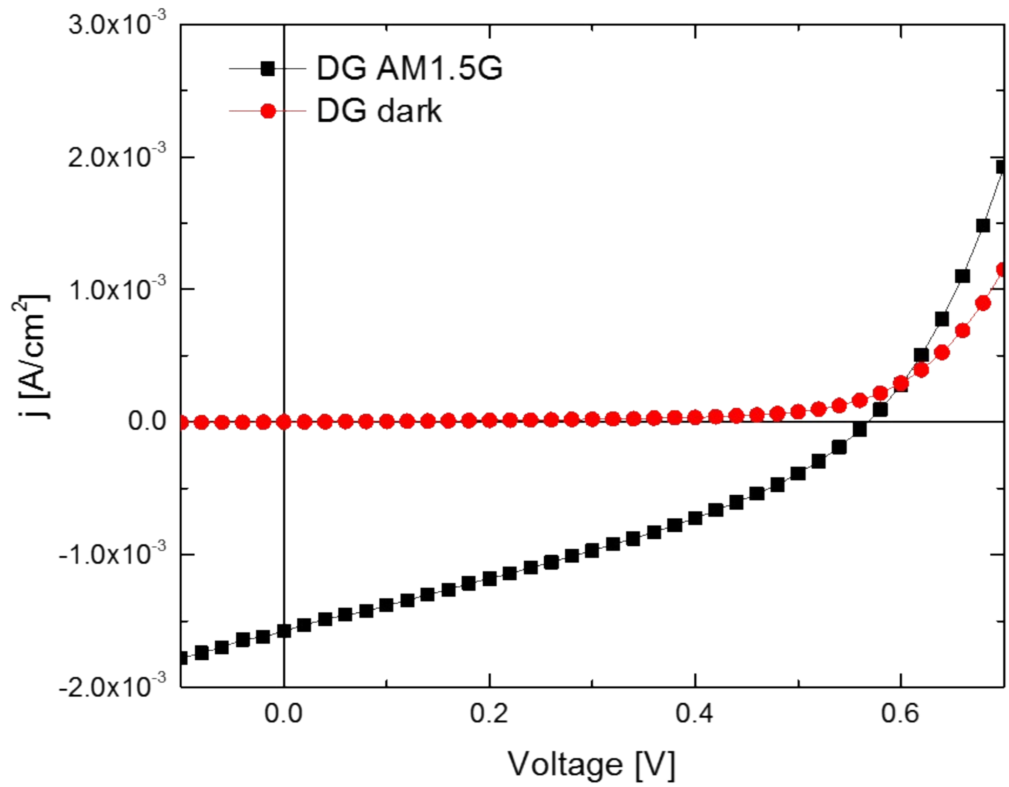

Figure S27. *J-V* curve for DG homojunction device with structure glass/ITO/PEDOT:PSS/**DG** (80 nm)/Sm/Al (PCE 0.3 %)